

CO₂/SO₂ emission reduction in CO₂ shipping infrastructure

Adeola Awoyomi^a, Kumar Patchigolla^a, Edward J. Anthony^a

^aSchool of Water, Energy and Environment (SWEE), Cranfield University, Cranfield, Bedfordshire MK43 0AL, UK.

Abstract

There is an increased focus on the reduction of anthropogenic emissions of CO₂ by means of CO₂ capture processes and storage in geological formations or for enhanced oil recovery. The necessary link between the capture and storage process is the transport system. Ship-based transport of CO₂ is a better option when distances exceeds 350 km compared to an offshore pipeline and offers more flexibility for transportation unlike pipelines which require a continuous flow of compressed gas. Several feasibility studies have been undertaken to ascertain the viability of large-scale transportation of CO₂ by shipping in terms of the liquefaction process, and gas conditioning, but limited work has been done on reducing emissions from the ship's engine combustion.

From 2020, ships operating worldwide will be required to use fuels with 0.5% or less sulphur content (versus 3.5% now) or adapt adequate measures to reduce these emissions. This study explores the use of the solvent-based post-combustion carbon capture and storage (CCS) process for CO₂ and SO₂ capture from a typical CO₂ carrier. A rate based aqueous ammonia process model was developed, validated, then scaled up and modified to process flue gas from a Wartsila 9L46F marine diesel engine. Different modes of operation of the carrier were analysed and the most efficient mode to operate the CCS system is while it is sailing. The heat recovered from the flue gas was used for solvent regeneration. A sensitivity study revealed that the 4 MW_{th} supplied by the "waste heat recovery" system was enough to achieve a CO₂ capture level of 70% at a solvent recirculation flowrate of 90-100 kg/s. The removal of SO₂ by the ammonia water solution was above 95% and this led to the possibility of forming a value-added product, ammonium sulphate. The boil-off gas and captured emitted CO₂ were recovered using a two stage re-liquefaction cycle and re-injected into the cargo tanks; thereby reducing extra space requirements on the ship.

Keywords: CCS, post-combustion carbon capture; chemical absorption; on-board carbon capture; marine propulsion engine; emission control

1. Introduction

The International Energy Agency has provided a list of technologies under the 2°C scenario (2DS) that would be needed to keep the global temperature rise below 2°C [1]. These technologies includes energy efficiency, renewables and carbon capture and storage (CCS). CCS technologies amongst others are expected to play a significant part in response to the climate change goal. It is the only approach capable of delivering significant emissions reduction from the use of fossil fuels for industrial purposes [1]. This requires both capture and transport of CO₂ from large point sources to storage, but the important variable is the distance between the source and sink [2]. Pipeline seems to be the best means of transportation for large amounts of CO₂ but lacks the flexibility for decarbonising numerous sources and is more expensive for long distances. Ship-based transport of CO₂ is a better option when the distance exceeds 350 km and, moreover, offers more flexibility in terms of quantity, shorter project durations, location of source and sink, and the distance to be transported [2,3]. The cost effectiveness of shipping CO₂ relative to alternative CO₂ transport options has been dealt with extensively elsewhere [4–8], but analysis on the reduction of CO₂ emissions from combustion ship fuel is limited. Although in most cases, CO₂ emissions are below 2% of the amount of CO₂ transported (assuming Liquefied Natural Gas (LNG) as the fuel type), higher

emissions can result due to very small ship size, high number of trips and longer distances [9]. Nearly all shipping-related flue gas emissions occur within 400 km of land [10], causing morbidity and death to nearly 3.7 million people in 2012 for example [11]. Also, the pollutant emissions can travel over hundreds of kilometres thus affecting inland air quality. The shipping industry is currently under increasing pressure to act upon the International Maritime Organisation (IMO) target of reducing greenhouse gas (GHG) emissions to 50% of 2008 levels by 2050 [12]. One vital step in meeting the target is to consider alternative fuel sources or expanding the potential for carbon capture while using fossil fuels [13].

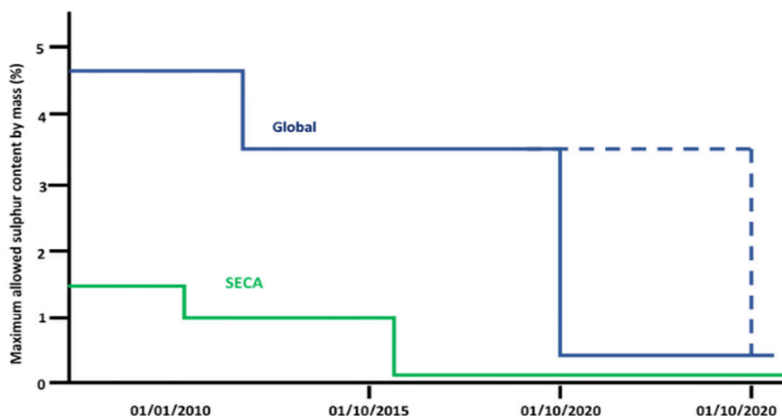


Figure 1: Sulphur content limits in bunker fuels [8,9]

Marine fuel combustion currently contributes approximately 3% and 13% of global man-made CO₂ and SO₂ emissions, respectively [16–18]. Most sea-going vessels still use heavy fuel oil (HFO) and marine gas oil (MGO), with a maximum sulphur limit of 3.5% for HFO and 0.1% for MGO [15]. The use of these fuels depends on the regions/routes in which the ship operates, as some regions have stricter limits on sulphur emissions than others. These stricter regions are called sulphur emission control areas (SECAs). Looking ahead to 2020, the IMO's Marine Environmental Protection Committee agreed to place a global sulphur content limit on bunker fuels of 0.5% (from 3.5%), as shown in Figure 1 [15]. This 0.5% sulphur limit and the recently adopted IMO initial GHG strategy to reduce CO₂ emissions by half in 2050 have the potential to spur on innovations and alternatives that will enable the shipping industry to meet the challenges ahead [19].

The need for alternative fuel options such as LNG, LPG, methanol, biofuel and hydrogen are likely to grow due to the IMO 2020 sulphur limit, but this will require sufficient production, availability of bunkering infrastructure and extensive on-board/engine modifications [20]. The use of LNG is currently increasing but the global LNG-fuelled fleet is still very small, hence the need for a post combustion capture solution. IMO introduced an alternative to fuel switching for the 2020 sulphur limit, the use of exhaust gas after-treatment scrubbers. This allows the continuous use of cheap/high-S fuels (HFO) while still meeting the stricter restrictions. Scrubbing is not a new option for land use and this technology has also been initiated for ships. One advantage of this is that it can be installed on existing vessels without replacement of ship engines. Dry and wet scrubbers are already in use in the marine market

Nomenclature

IMO	International Maritime Organisation	HFO	Heavy fuel oil
LNG	Liquefied natural gas	LPG	Liquefied petroleum gas
SECA	Sulphur emission control areas	BOG	Boil-off gas
MDO	Marine diesel oil	MGO	Marine gas oil
LCO ₂	Liquefied carbon dioxide	WHRS	Waste heat recovery system
PCC	Post-combustion capture	CCS	Carbon capture and storage
Sim	Simulation	Exp	Experimental

Diff	Absolute difference	GHG	Greenhouse gas
------	---------------------	-----	----------------

Monoethanolamine is regarded as the reference chemical solvent for post-combustion capture of CO₂, but is easily degraded by oxidants (SO₂, NO₂ and O₂), corrodes equipment and requires high energy consumption in the regeneration step [21]. The absorption of CO₂ is also reduced by an irreversible reaction with SO₂ [22]. As a result, SO₂ concentrations should be less than 10 ppm for amine-based solvents [23]. Conventional techniques for removing CO₂ and SO₂ individually are not cost effective for marine operations; the additional capital, energy, and operational costs of these techniques are currently prohibitive, and it may, therefore, be advantageous to consider a solvent that can remove both CO₂ and SO₂.

Researchers have explored the use of aqueous ammonia to simultaneously remove multi-components such as CO₂ and SO₂ from flue gases [23–27]. The use of ammonia is beneficial due to its low heat requirement (less energy penalty) for regeneration, low chemical cost, thermal stability, ability to release CO₂ at higher pressures, saleable by-products and tolerance to O₂ and contaminants, as compared to conventional amines [28–32]. There are two variations of the ammonia process: the first is the chilled ammonia process (CAP) developed by GE [26,33,34]; and the second is the aqueous ammonia process offered by the Powerspan ECO₂ process [35]. In the chilled ammonia process, the absorption of CO₂ is carried out under refrigerated conditions (0–20°C, preferably 10°C) while in the aqueous ammonia process, absorption occurs above 20°C. A pilot trial conducted by CSIRO and Delta Electricity using aqueous ammonia at the Munmorah coal power plant confirmed the technical feasibility and benefits of using aqueous ammonia [36,37] for both CO₂ and SO₂ removal. Although the disadvantage of ammonia noted in the pilot trials study is the slow kinetics for CO₂ absorption and its high volatility (slip challenge).

Modelling studies have also been carried out to quantify the performance of multi-pollutant capture processes using aqueous ammonia. A number of researchers have developed models using the rate-based approach for CO₂ capture and validated the model using experimental results, including those from the Munmorah pilot-plant trials [36–41]. Li et al. [38] proposed a new model to combat the ammonia slip using a rate-based modelling approach. It combines SO₂ and CO₂ removal with NH₃ recycling as shown in Figure 2. The process consists of a pre-treatment column, an NH₃ wash column, and then a typical CO₂ capture process. The NH₃ vaporised from the CO₂ absorber is absorbed in the wash column and the NH₃-rich solution collected at the bottom of the wash column enters into the pre-treatment column. The SO₂ is absorbed by the NH₃-rich solution entering the pre-treatment column, and the NH₃ is stripped by the high-temperature flue gas. The process offers SO₂ removal and NH₃ reuse efficiencies of above 99.9%, and is adaptable to different scenarios involving high SO₂ levels in the flue gas and high NH₃ levels from the CO₂ absorber [38].

The motivation of this paper is to explore the use of the solvent-based post-combustion capture (PCC) process using aqueous ammonia to reduce CO₂ and SO₂ emissions from a typical CO₂ carrier. This is to be done through modelling of the ship's energy system integrated with the capture system. The Munmorah pilot plant is used as the reference case, together with a rate-based model in Aspen PlusTM V10. Here, the following procedures were carried out:

- Quantification of shipping emissions through the model development of the ship's energy system under different modes of operation.
- Steady state process development of the NH₃ capture process and CO₂ liquefaction process.
- Integrated model performance of both models at different operating conditions.

2. Marine emission reduction

Mitigation measures for ship pollution were classified into three strategies [42], namely, technical, operational, and market-based strategies. The technical strategy includes upgrading or retrofitting older ship engines with more efficient or low-emitting systems. The operational strategy involves reducing emissions by modifying how vessels operate while docking or entering the harbour. The market-based strategies are emissions trading programs put in place to make polluters pay a fair price for pollutions, in order to spur on both operational and technological

2.3 CCS technology advancement for ships

There are a few studies in the public domain on the integration of capture systems on ships, most of which are based on post-combustion capture. Process System Engineering group and Det Norske Veritas carried out a concept design for on-board carbon capture, liquefaction and temporary storage of CO₂ for ships. The results estimated that the process is feasible and capable of reducing maritime CO₂ emissions by 65% [50]. No further details regarding the process engineering are available in the public domain. Due to the constant movement constraint of marine vessels, a solidification method for CO₂ storage on board was proposed for separating CO₂ emissions from exhaust gases [51]. The CO₂ gas is absorbed by sodium hydroxide to form sodium carbonate, which is then treated with quicklime in solution to form solid calcium carbonate, which can be stored safely on board or unloaded at the destination.

Luo and Wang [52] recently developed a solvent-based PCC process to capture CO₂ from the energy system in a typical cargo ship. It was found that a carbon capture level of 73% was obtained when the ship's energy system was integrated with the PCC process due to a limited supply of heat and electricity. Addition of a gas turbine increased the capture level to 90%. Another study was carried out on a LNG-fuelled vessel; CO₂ was captured from the exhaust gases on board [53]. The vessel was lengthened by 6 m to accommodate the CCS system [53]. Apart from these studies mentioned above, no other publication appears to be currently available; therefore, a need exists to further the level of understanding of the effects of capture system integration on a ship.

3. Re-liquefaction of CO₂ boil-off gas (BOG)

When transporting liquefied CO₂ (LCO₂), BOG is generated. The BOG is the vapour produced due to ambient heat penetration into the cargo tanks caused by a significant temperature difference. The rate of BOG is also affected by sea conditions, cargo tank content (level of impurities), tank design pressure, and different operational modes [54]. Based on theoretical calculations, there is 0.1-0.15% of the cargo capacity boiled off per day, which over a 21 d voyage would be a significant amount for LNG carriers [55]. For CO₂ carriers, no detailed model is available to predict the BOG. The BOG of LCO₂ carriers has been estimated to be 0.15% per day from LNG ships by comparing physical properties such as heat of vaporisation and density including the size of the tank [56]. The volume of LCO₂ is about 1/600 that of gaseous CO₂ under normal conditions and hence substantially larger quantities can be stored on board. In Figure 3, the widely accepted operating conditions of the LCO₂ transport ship vary between -20°C to -50°C. The corresponding density of the liquid at -50°C and -20°C is 1154.6 kg/m³ and 1031.7 kg/m³ respectively, meaning 12% more cargo is stored at -50°C than at -20°C. Semi-pressurised ships are designed for a working pressure of 5-7 bara and operate at low temperatures (-48°C for LPG (propylene)). They can be retrofitted for CO₂ transport due to similar cargo conditions [4]. Figure 4 shows a schematic diagram of a two stage direct compression cycle (open cycle), where the BOG is compressed, cooled and expanded before being re-injected into the tanks. In this study, a two stage re-liquefaction cycle was used for both the BOG and captured CO₂ gas. This has been considered feasible for CO₂ carriers in previous studies [57–59].

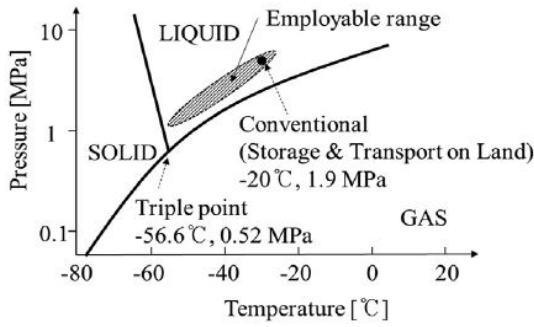
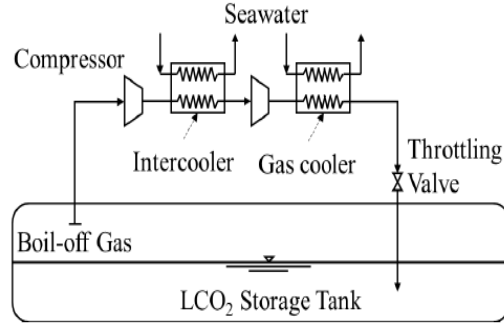
Figure 3: CO₂ phase diagram [52]

Figure 4: Two-stage direct compression cycle [49]

4. Estimating ship emissions

4.1 Reference CO₂ vessel

To transport large amounts of CO₂, pipelines seem to be the best solution. But transporting CO₂ by ship will be far more flexible and less expensive for long distances. There are ships available for transporting carbon dioxide for use in industry but they typically have small capacities: between 800 and 1200 m³ [2]. Economic large-scale transport of CO₂ by ship can be done in a semi-pressurised vessel at conditions near the triple point [60]. A combined LPG/CO₂ semi-refrigerated ship was chosen for a complete transport chain of CO₂ between capture and storage, with a storage capacity of 20,000 m³ at −52 °C and 6.5 bar for complete energy and cost analysis [2]. Therefore, for this study, the chosen reference vessel is a LPG semi-refrigerated vessel (Table 1) with a storage capacity of 20,550 m³ close to the same storage conditions as those specified by Decarre et al. [2].

4.2 Model development of Diesel Engine and Waste Heat Recovery System (WHRS)

4.2.1 Diesel engine

The ship's energy system consists of a propulsion system, auxiliary generators and a waste heat recovery system for energy efficiency. The prime mover, the main engine, is the main source of propulsion for a ship. It converts the chemical energy in the fuel into mechanical work, by generating the thrust for driving the ship. According to Luo and Wang [52], the thermal process occurring in the cylinders is a critical factor for model development. The engine for the reference CO₂ carrier was chosen from Wartsila (9L46F marine diesel engine) to provide propulsion and electrical power to meet the capacity as specified in Table 1. The type of fuel consumed by the engine is HFO, with a sulphur content of 3.29% as shown in Table 2. In the model development of the engine (Figure 5), the Peng-Robinson equation of state with Boston-Mathias modifications (PR-BM) property method was used to predict the performance [52]. The thermal process was split into three main blocks: compression, combustion and expansion in Aspen Plus™ V10. For the validation, at different loads, the model was compared to the Wartsila 9L46F engine handbook performance data [61]. Most of the results appear to be in good agreement when compared with the engine data and Luo and Wang's model [52] as shown in Table 3. After validation, the model air and gas flowrates were adjusted to the specification of the ship requirements as shown in Table 4. Different modes of operation were considered in the model: sailing, manoeuvring and hoteling mode. The sailing, manoeuvring and hoteling are achieved at 85%, 75% and 50% of full engine power, respectively.

Table 1 Characteristics of the reference LPG carrier [62]

Item	Value
Size (m ³)	20550
Sailing speed (knot)	16

Table 2: Elemental Analysis of HFO [63]

Element	HFO (%wt)
Carbon	85.00
Hydrogen	10.89

Length (m)	160	Oxygen	0.03
Beam (m)	25.60	Nitrogen	0.24
Depth (m)	16.40	Sulphur	3.29
Draft (Tropical) (m)	11.15		
Propulsion power (kW)	7860		
Auxiliary power (kW)	2340		

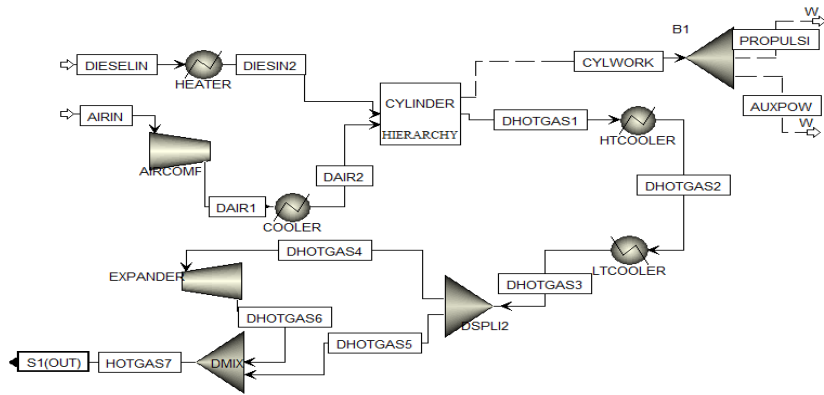
Figure 5: Model flowsheet of the diesel engine in Aspen PlusTM V10 [52]

Table 3: Validation of the Aspen Plus diesel engine model performance

Load (%)	Fuel flowrate (kg/s)	Air flowrate (kg/s)		Engine output (kW)	Fluegas flowrate (kg/s)
100	0.539	18.80	Handbook	10800	19.62
			Model	10838.89	19.34
			Wang's model	10805	19.34
			Deviation-handbook(%)	-0.36	1.431
			Deviation-Wang's model(%)	0.31	0
85	0.442	15.98	Handbook	9180	17.10
			Model	9215	16.40
			Wang's model	8905	16.40
			Deviation-handbook (%)	-0.38	4.090
			Deviation-Wang's model(%)	3.36	0
75	0.401	14.10	Handbook	8100	16.20
			Model	8129.67	14.50
			Wang's model	8062	14.50
			Deviation-handbook(%)	-0.37	10.50
			Deviation-Wang's model(%)	0.83	0
50	0.270	9.40	Handbook	5400	11.16
			Model	5419.18	9.670
			Wang's model	5477	10.57
			Deviation-handbook(%)	-0.36	13.33
			Deviation-Wang' model(%)	-1.07	-9.30

Table 4: Diesel engine model data specifications without the capture

Load (%)	Fuel flowrate (kg/s)	Air flowrate (kg/s)	Engine output (kW)	Flue gas flowrate (kg/s)
100	0.50	17.70	10200	18.20
85	0.42	15.02	8670	15.44
75	0.35	13.30	7650	13.65
50	0.27	08.90	5100	09.17

4.2.2 Waste Heat Recovery System

Most marine diesel engines are about 50% efficient in the utilizing the heat energy generated and the remainder is lost as waste heat [64]. Utilizing the “waste heat” energy can increase plant efficiency and reduce the need to burn more fuel. This can be done by using a WHRS to produce power or heat [65]. A WHRS was integrated with the diesel engine to make use of waste heat thereby increasing efficiency. The diesel engine and the WHRS fully represents the ship energy system. The heat extracted is used to produce superheated steam and this serves as thermal energy for solvent regeneration, thus reducing the need for additional fuel consumption. The model was developed in Aspen PlusTM V10 with the STEAMNBS property method for the accurate evaluation of the steam properties [52]. From preliminary calculations, the thermal energy recovered from the flue gas is dependent on the engine load (Figure 6). The optimal mode for operating is at sailing and manoeuvring in order to make use of the high thermal energy produced.

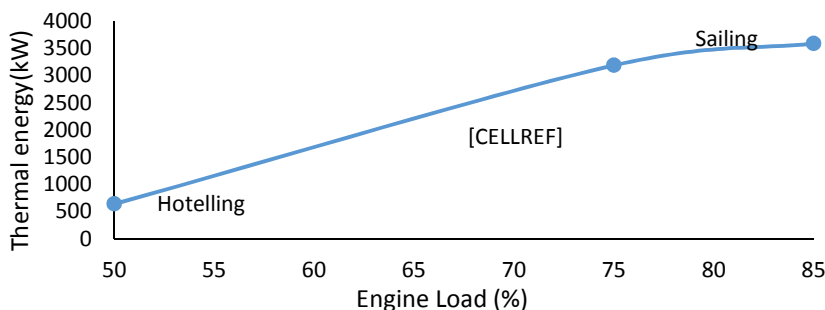


Figure 6: Flue gas thermal energy capability at each mode of operation

4.3 Ship case study

For a CCS system to be integrated on a ship, the amount of carbon emissions must be known to adequately design the required size of the solvent tank and storage system. The amount of carbon emissions depends on the amount of fuel consumed and the distance/duration of the sailing route. In this scenario, a ship sailing from Mawei Port (China - **A**) to Port of Aardalstangen (Norway - **B**) was selected [66] (Figure 7) and with an assumed capacity of an LPG carrier. The LPG carrier is called the Navigator Aries with a capacity of 20550 m³ [62]. It has been suggested that an existing LPG ship could be repurposed for CO₂ shipping, or ships could be built in such a way that they could be operated for transporting CO₂ as well as LPG [2,9,67]. The average distance of the selected sailing route is approximately 22700 km with a sailing speed of 16 knots results in an approximate crossing time of 32 d. During sailing, it was assumed that the marine engine operated at both 85% and 75% of full power respectively and the effect of weather conditions was neglected. Here, 60% of the journey time was assumed to be spent sailing while the remaining time was either in port or at anchor [68].



Figure 7: Map route from Mawei Port (China) to Port of Ardalstangen (Norway)

5. Model and liquefaction process

development for CCS

5.1 Process Description

The design of the pilot plant at the Munmorah coal power station and the results presented by Hu et al [36,37] are used in this work as the basis for the process design. The process consists of one pre-treatment column, two absorber columns with individual wash column at the top, stripper and a heat exchanger (Figure 8). The flue gas flows into the pre-treatment column for SO₂ removal and cooling, afterwards it is directed into the absorber from the bottom and the lean solvent from the top. The wash columns at the exit of the absorber serves as measure to prevent ammonia slip due to its volatility. There were two absorber columns operated either in series or parallel to allow for flexibility [37]. The columns were constructed with stainless steel pipe and are random packed with 16 or 25 mm Pall rings. The height and the inner diameter of the absorber are 7.8 m and 0.6 m, and for the stripper is, 3.5 m and 0.4 m respectively. The height and diameter of the wash columns are 1.7 m and 0.5 m and that of the pre-treatment column is 3.5 m and 0.5 m respectively. Flue gas flowrate varied from 650-1000 kg/h while the lean solvent flowrate was between 50-134 L/min. The gas pressure in the absorber was varied from 1.01-1.5 bar while stripper pressure was varied from 3-8.5 bar. In order to avoid precipitate formation in the absorber, the lean solvent temperature was maintained between 10-30 °C. The minimum regeneration energy obtained for the trials was at least 4-4.2 MJ/kg CO₂ due to the dilute content of aqueous ammonia in the process [37]. These pilot plant trials have been detailed by Hu et al. [36,37].

5.2 Model specification and validation

The rate based aqueous ammonia process model was developed in Aspen PlusTM V10 and validated with the Munmorah pilot plant data [37]. The pre-treatment, absorber and stripper columns were modelled using RateFrac units because absorption and regenerative process are more accurately simulated in terms of the material and energy balance, chemical kinetics, mass and heat transfer properties compared to the RadFrac model [69]. The Redlich-Kwong equation of state and the Electrolyte-NRTL thermodynamic method were used to compute the non-idealities in the vapour and liquid phase properties respectively. The flow model is counter current. Mass transfer coefficient and heat transfer coefficient is estimated from Bravo et al. [70] and Chilton-Colburn method [71]. Other relevant coefficients are obtained by the default correlations of the Ratefrac model in Aspen Plus.

The NH₃-CO₂-SO₂-H₂O chemistry system is defined by equilibrium reactions in Table 5 [24]. The equilibrium constants (*Keq*) of these reactions given on a molar concentration are temperature dependent and are defined as:

$$\ln Keq = A + \frac{B}{T} + C \cdot \ln\left(\frac{T}{[1 K]}\right) + D \cdot T \quad (1)$$

Where T is the temperature in Kelvin, constants A, B, C, D were adjustable parameters available in Aspen databank [72] except for the reaction (8) obtained from Ermatchkov et al. [73], and their units are: A is dimensionless, B has the dimensions of T, C is dimensionless, and D has the dimensions of T⁻¹.

Table 5: Chemical reactions and coefficients of equilibrium constants of the NH₃-CO₂-SO₂-H₂O system [24]

No	Reactions	A	B	C	D
1	$2\text{H}_2\text{O} \leftrightarrow \text{H}_3\text{O}^+ + \text{OH}^-$	132.899	-13445.9	-22.4773	0
2	$\text{CO}_2 + 2\text{H}_2\text{O} \leftrightarrow \text{H}_3\text{O}^+ + \text{HCO}_3^-$	231.465439	-12092.1	-36.7816	0
3	$\text{HCO}_3^- + \text{H}_2\text{O} \leftrightarrow \text{CO}_3^{2-} + \text{H}_3\text{O}^+$	216.049	-12431.7	-35.4819	0
4	$\text{NH}_3 + \text{H}_2\text{O} \leftrightarrow \text{NH}_4^+ + \text{OH}^-$	-1.2566	-3335.7	1.4971	-0.0370566
5	$\text{NH}_3 + \text{HCO}_3^- \leftrightarrow \text{NH}_2\text{COO}^- + \text{H}_2\text{O}$	-4.583437	2900	0	0
6	$2\text{H}_2\text{O} + \text{SO}_2 \leftrightarrow \text{H}_3\text{O}^+ + \text{HSO}_3^-$	-5.978673	637.395996	0	-0.0151337
7	$\text{H}_2\text{O} + \text{HSO}_3^- \leftrightarrow \text{H}_3\text{O}^+ + \text{SO}_3^{2-}$	-25.290564	1333.40002		0
8	$2\text{HSO}_3^- \leftrightarrow \text{S}_2\text{O}_5^{2-} + \text{H}_2\text{O}$	-10.226	2123.6	0	0
9	$\text{NH}_4\text{HCO}_3(\text{s}) \leftrightarrow \text{NH}_4^+ + \text{HCO}_3^-$	554.8181	-22442.53	-89.00642	0.06473205
10	$(\text{NH}_4)_2\text{SO}_3(\text{s}) \leftrightarrow 2\text{NH}_4^+ + \text{SO}_3^{2-}$	920.3782	-44503.83	-139.3449	0.03619046
11	$(\text{NH}_4)_2\text{SO}_3 \cdot \text{H}_2\text{O}(\text{s}) \leftrightarrow 2\text{NH}_4^+ + \text{SO}_3^{2-} + \text{H}_2\text{O}$	-1297.041	33465.89	224.2223	-0.3515832

The reaction rates (r) of the reaction (j) are presented in Table 6 below and are determined by the power law defined as;

$$r_j = k_j^0 \exp\left(-\frac{E_j}{RT}\right) \prod_{i=1}^N C_i^{a_{ij}} \quad (2)$$

Where k_j^0 represents the pre-exponential factor for the reactions (j) (kmol/m³ s), T is the absolute temperature (K), E_j is the activation energy (J/kmol); R is the universal gas constant (J/kmol K); C_i is the molarity of component i (kmol/m³) a_{ij} is the stoichiometric coefficient of component i in the reaction j . The power law parameters were obtained from the work of Pinsent et al. [74,75] and are applied to the rate-based model with the Munmorah pilot-plant data. Hanak et al. [41] noted that the Pinsent et al. [74,75] kinetic parameters provided close model prediction of the Munmorah pilot plant data when compared with the work of Puxty et al. [29] and Jilvero et al. [76].

Table 6 Kinetic parameters ' k_j^0 ' and ' E_j ' for the reactions in the NH₃-CO₂-SO₂-H₂O system

No	Reaction	Parameters	
		k_j^0 (kmol/m ³ s)	E_j (J/kmol)
1	$\text{CO}_2 + \text{OH}^- \leftrightarrow \text{HCO}_3^-$	4.32e+13	5.55e+7
2	$\text{HCO}_3^- \leftrightarrow \text{CO}_2 + \text{OH}^-$	2.38e+17	1.23e+8
3	$\text{NH}_3 + \text{CO}_2 + \text{H}_2\text{O} \leftrightarrow \text{NH}_2\text{COO}^- + \text{H}_3\text{O}^+$	1.35e+11	4.85e+7
4	$\text{NH}_2\text{COO}^- + \text{H}_3\text{O}^+ \leftrightarrow \text{NH}_3 + \text{CO}_2 + \text{H}_2\text{O}$	4.75e+20	6.92e+7

Table 7: Comparison of key parameters of the capture process between the model and the pilot plant

TEST		Lean NH ₃ Conc (wt%)	Lean solvent flow rate (L/min)	CO ₂ absorption rate (kg/h)	CO ₂ removal efficiency (%)	CO ₂ lean loading (mol/mol)	CO ₂ rich loading (mol/mol)	Reboiler duty (kW)	Stripper bottom temp (°C)
32	Exp	3.6 ± 0.4	134	76 ± 5	61.7	0.24 ± 0.03	0.37 ± 0.03	111	129.7
	Sim	3.6	134	80.3	66	0.28	0.4	108	129.7
	Diff	0	0	-4.3	-4.3	-0.04	-0.03	3	0
32B	Exp	3.9 ± 0.2	134	80 ± 4	71.4	0.22 ± 0.02	0.32 ± 0.03	111	131.6
	Simu	3.7	134	82	72.2	0.22	0.34	115	132.0
	Diff	0.2	0	-2	-0.8	0	-0.02	-4	-0.4
31	Exp	4.08 ± 0.1	134	80 ± 2	80.2	0.24 ± 0.01	0.32 ± 0.03	111	131.6
	Sim	4.08	134	79.8	80.5	0.24	0.34	112	132.0
	Diff	0	0	0.2	-0.3	0	-0.02	-1	-0.4

The rate based model performance was compared with three pilot test cases to confirm its validity. The simulation model consists of the pre-treatment column, absorber (double height, to depict the two columns), stripper, heat exchanger and the wash column (Figure 9). The NH_3 vaporised from the CO_2 absorber is absorbed in the wash column, the NH_3 -rich solution (ammoniated water) collected at the bottom of the wash column enters into the pre-treatment column. The SO_2 is absorbed by the NH_3 -rich solution entering the pre-treatment column. It was concluded that the prediction of the CO_2 absorption process performance agrees well with the experimental plant data (Table 7), although there were some deviations of key parameters in the model. SO_2 removal efficiency from the pre-treatment column was above 95% for each case validated which is in agreement with the pilot plant data.

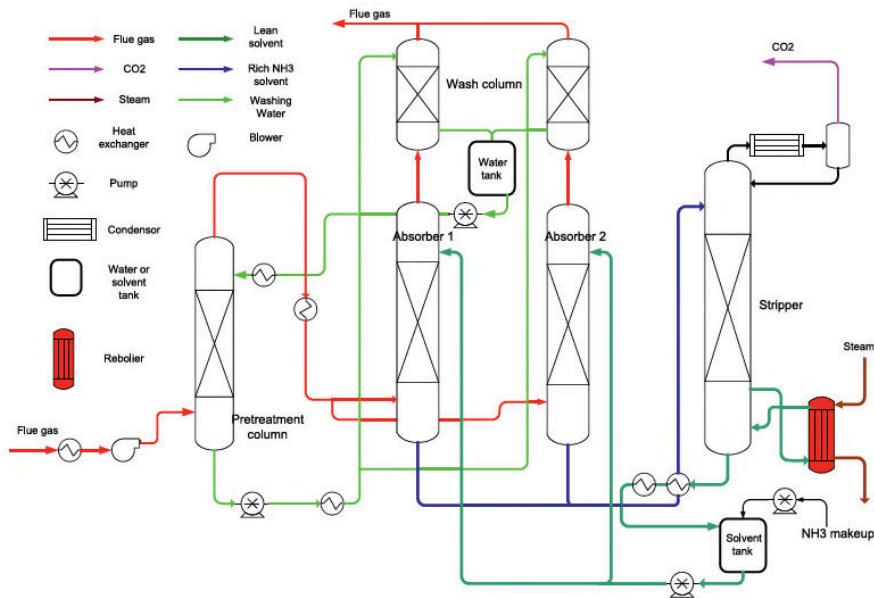


Figure 8: Simplified flowsheet Munmorah pilot plant with operation of two parallel columns [17]

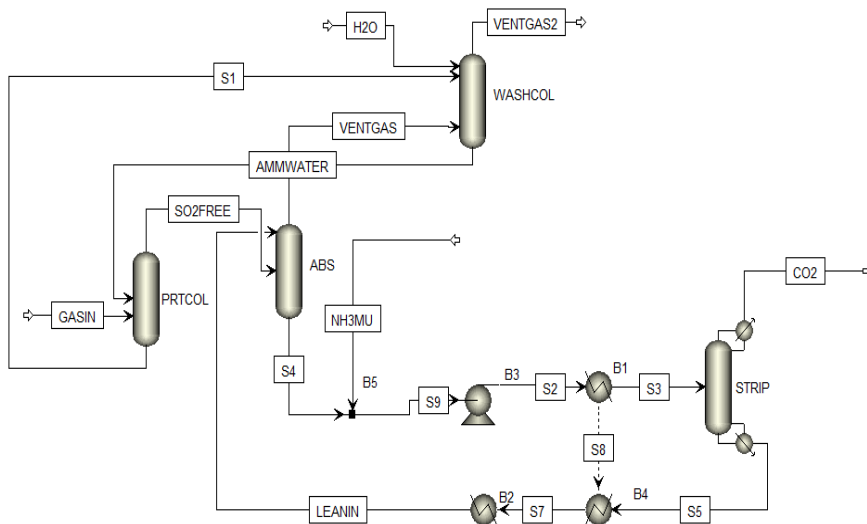


Figure 9: Model for the capture process in Aspen plus™ V10

5.3 Process scale up and modification

The model was scaled up to capture 75% of CO₂ from the flue gas of the ship's energy system using 4.1% aqueous ammonia solution. The scaling up was done using the methodology described by Kister [77]. The operating region of a packed column is limited by the flooding and minimum liquid load [78]; therefore an efficient packed column design should be characterised by a good liquid and gas distribution that is achievable by operating at an economical pressure drop. The pressure drop values for the absorber and stripper was selected to be of 42 mmH₂O/m of packing; which is within the recommended values 15 and 50 mmH₂O/m proposed by Sinnott and Towler [79]. Pall packing was used as stated in the pilot plant study. The required solvent flow rate was estimated based on the conditions specified in Table 8. The lean and solvent loadings from the pilot plant study were used for the full-scale calculations. The generalised pressure drop correlation was used to calculate the cross-sectional area of the absorber and stripper. The calculated values were used as initial guesses with operating conditions set in order to prevent column flooding exceeding 80%. The capture process model was modified by addition of a wash column at the outlet of the stripper in order to reduce ammonia spillage (Figure 10). Ammonia recovered from the flue gas in the wash column is used to capture SO₂ in the pretreatment column. This reaction forms ammonium sulphite but in dilute concentrations. A packed column reactor which serves as a crystallisation unit was included after the precipitate was formed and separated out in a centrifuge. The remaining liquid left after the separation was injected into the wash columns for ammonia slip removal. Due to unavailability of kinetic information, the reactor was modelled as a stoichiometric reactor where (NH₄)₂SO₃ was obtained from the stoichiometry in which 80% conversion of SO₃²⁻ is achieved. The packing heights of the absorber and stripper are 10 m and 6 m respectively; which is much shorter than typical ones installed onshore. The main parameters characterising the developed full-scale capture process are in Table 9.

5.4 Re-liquefaction of boil-off gas (BOG) and captured CO₂

A re-liquefaction cycle was simulated for both the BOG and captured CO₂ using an open loop cycle as shown in Figure 11. The BOG and captured gas are compressed, cooled and expanded in the cycle before being piped back into the cargo tanks. The BOG rate assumed for this study is 0.2%/day and can be calculated with the formula [80];

$$BOG \text{ rate} = \frac{\text{Heat flow} * 24h * 3600}{(\rho_{CO_2} * V_{CO_2} * L_{CO_2})} \quad (3)$$

Where ρ_{CO_2} is the density of CO₂ (kg/m³) at a specific temperature (°C); V_{CO_2} is the volume of CO₂ (m³) and L_{CO_2} is the latent heat of vaporisation (kJ/kg); heat flow represents the heat ingress into the cargo tank. Table 10 lists the cycle parameters of the present study; assuming pure CO₂ conditions.

Table 8: Calculation of the required lean solvent flow

Description	Value
Flue gas mass flow rate (kg/s)	15.44
Flue gas CO ₂ composition (%wt.)	8.50
Flue gas SO ₂ composition (%wt.)	0.18
Flue gas H ₂ O composition (%wt.)	2.60
Flue gas N ₂ composition (%wt.)	77.02
Flue gas O ₂ composition (%wt.)	11.7
Captured CO ₂ flowrate (kg/s)	0.98
Lean solvent mass fraction, NH ₃ (%wt.)	4.1
Estimated lean solvent circulation rate (kg/s)	140

Table 9: Base case parameters for the fully developed capture plant

Description	Value	Description	Value
CO ₂ capture rate (%)	75	Reactor type	RSTOIC
SO ₂ capture level (%)	90	Reactor diameter (m)	2

Absorber diameter (m)	5	Reactor height (m)	7
Absorber packing height (m)	10	Absorber pressure (bar)	1
Absorber packing type	Pall ring (25mm)	Pre-treatment column pressure (bar)	1
Pre-treatment column diameter (m)	0.5	Stripper pressure (bar)	6
Pre-treatment column packing height (m)	3	Wash column pressure (bar)	1
Pre-treatment column packing type	Pall ring (25mm)	Condenser temperature (°C)	25
Stripper diameter (m)	2	Reboiler temperature (°C)	132
Stripper packing height (m)	6	Specific reboiler duty (MJ _{th} /kgCO ₂)	4.5
Stripper packing type	Pall ring (25mm)	CO ₂ purity (%)	90
Number of wash columns	2	Lean solvent (wt %)	4.1
Wash column packing type	Pall ring (16mm)	Lean solvent temperature (°C)	26
Wash column diameter (m)	0.5		
Wash column packing height (m)	3		

Table 10: Re-liquefaction cycle specification

Parameter	Value	Parameter	Value
Composition	100% CO ₂	BOG flow (kg/s)	0.55
Volume of CO ₂ tank (m ³)	20550	Captured CO ₂ flowrate (kg/s)	0.74
BOG rate (%/day)	0.2	LCO ₂ tank temperature (°C)	-50
BOG temperature (°C)	-50	LCO ₂ tank pressure (bar)	7
Latent heat of vaporisation of CO ₂ at -50°C (kJ/kg)	339.7	Sea water temp (°C)	10
Density of CO ₂ at -50°C (kg/m ³)	1154.6		

Table 11: Simulation results of the capture plant process

Stream	GASIN	LEANIN	H2O	VENTGAS	VENTGAS2	PRODUCTS	SOLIDS	LIQGAS	H2O2	CO2CAP	S5
Temperature (°C)	70	26	10	26	32	30	35	35	10	11	132
Pressure (bar)	1.013	6	1.03	1.03	1.013	1.013	2	1	1.013	5.95	6
Mass flow (kg/s)	15.44	140	200	13.20	13.08	1512.47	0.12	1512.35	15	0.74	140
NH ₃ emissions (ppm)	-	-	-	21970	40	-	-	-	-	<0.001	-

Table 12: Simulation results for two-stage BOG and CO₂ captured re-liquefaction

Stream	BOG	CO2CAP	1	2	3	4	5	6	7	8
Vapor fraction	1	1	1	1	1	1	0	0.44	1	0
Temperature (°C)	-50	11	-33	117.8	15	72	15	-50	-50	-50
Pressure (bar)	7	6	6	31.76	31.56	57.46	57.26	7	7	7
Mass flow (kg/s)	0.55	0.74	2.63	2.63	2.63	2.63	2.63	2.63	1.34	1.29

5. Integrated ship model

The linked ship energy system and capture plant is called the integrated ship model. The linkage of both models involves the following;

- Flue gas stream from the ship energy system to the WHR
- Direct contact cooling of the flue gas from the WHR to the pre-treatment column
- Thermal energy from the WHR used to regenerate the solvent in the reboiler

In the integrated ship model, it is assumed that all the NO_x and particulate matter are removed upstream of the absorber and the direct contact cooler is further used to reduce the flue gas temperature to 70°C. The cooled flue gas

The diagram illustrates the process flow of a CO₂ capture plant. The process involves several unit operations and streams:

- Inputs:** CO₂CAP and BOG feed into a compressor (B4).
- Stream 1:** Output of B4, entering COMP1.
- Stream 2:** Output of COMP1, entering COOLER.
- Stream 3:** Output of COOLER, entering COMP2.
- Stream 4:** Output of COMP2, entering COOLER2.
- Stream 5:** Output of COOLER2, entering valve B2.
- Stream 6:** Output of B2, entering separator SEP.
- Stream 7:** Output of SEP, entering B4.
- Stream 8:** Output of SEP, exiting the process.
- Other Features:** A vent stream exits the process near the BOG input, and a product stream exits the process near the SEP output.

Figure 11: Simulation model of BOG and captured CO₂ re-liquefaction

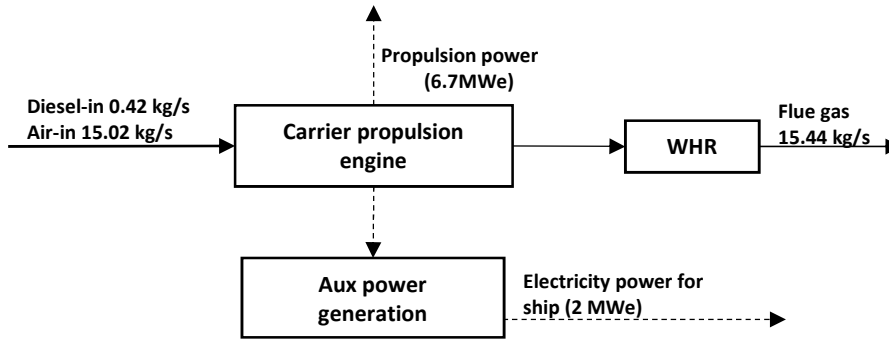


Figure 12: Reference case scenario at 85% load without capture

6.1 Performance of the ship energy system with the capture plant

The performance of the ship model integrated with the post-combustion capture plant was investigated in this section. The integrated plant model was simulated at steady state. Power requirements for the CCS system, that is for compressing CO_2 for storage and the capture system are assumed to be 1 MWe. Three case studied are considered; one involves the effect of the lean solvent flowrate, the next investigates the effect of two different NH_3 solvent concentrations and the last is the effect of speed change on the process performance.

1) Effect of lean solvent flowrate on process performance

In this analysis, the lean solvent flowrate was varied at a fixed engine load and solvent concentration of 4.1 wt%. Other parameters that influence the process performance like pressure, height and diameter were also kept constant. Figure 14 illustrates the effect of changing the lean solvent flowrate on the capture level and reboiler duty at 85% engine load. It highlights that an increase in lean solvent flowrate increases the capture level and reboiler duty. The solvent flowrate was varied from 70 – 300 kg/s; resulting in an increased capture level of 65 – 80 % respectively. For the 4 MW_{th} recovered thermal heat from the WHR, a capture level of 70% and lower can be achievable. To attain higher capture level, additional power would have to be supplied.

2) Effect of change in NH_3 concentration

The integrated ship model performance at two different concentrations of NH_3 is shown in Table 13. The fuel burn rate was increased in order to maintain the required speed needed at 85% load while CCS is in operation for a

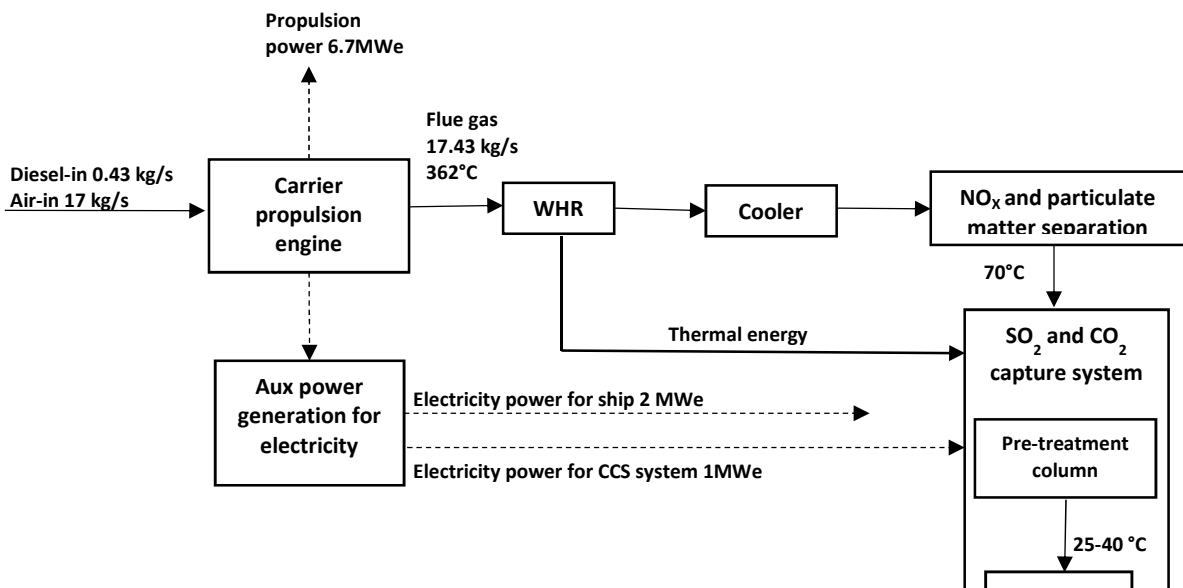


Figure 13: Linking the flue gas from the ship energy system with capture plant at 85% load

capture level of 75%. In summary, an increase in the NH_3 concentration resulted in reduced solvent regeneration duty and flowrate. At 3.5 wt% NH_3 concentration, the heat duty demanded by the reboiler (6.3 MJ/kg- CO_2) and flowrate (250 kg/s) increased to raise the temperature of the circulated solvent to the required set point (sensible heat). Here, the amount of pure ammonia required is reduced. For the 4.1 wt%, the heat duty required was reduced (4.5 MJ/kg- CO_2) and also the solvent flowrate (140 kg/s). With the NH_3 concentration increase, the NH_3 concentration in the exit gas increased compared to that at lower concentration, thereby leading to an increase in extra energy requirement for the NH_3 abatement system. For the actual CO_2 process, a trade-off would need to be determined based on the effect on the capture process or the NH_3 abatement system [81].

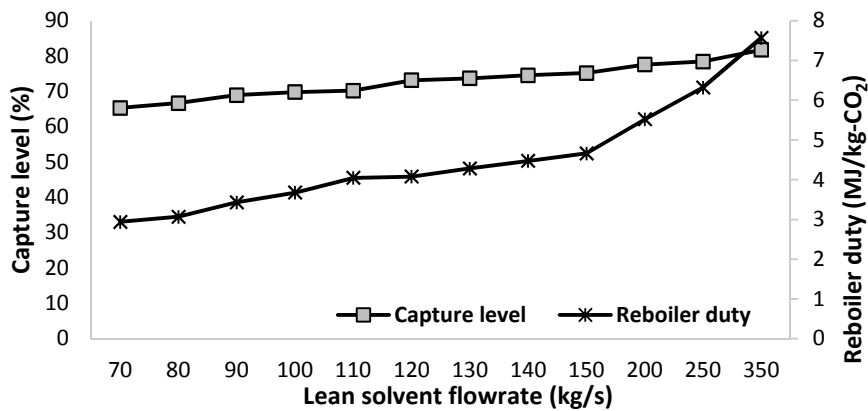


Figure 14: Effect of lean solvent flowrate on reboiler duty and capture level at 85% load

Table 13: Parameters summary for the integrated ship model with and without CO_2 capture at different NH_3 concentrations at 85% load

Description	Without CO_2 capture	With CO_2 capture (3.6 wt% NH_3)	With CO_2 capture (4.1 wt % NH_3)
CO_2 capture level (%)	0	75.00	75.00
Flue gas rate (kg/s)	15.44	17.43	17.43
Solvent circulation flowrate (kg/s)	0	250	140
Lean/rich loading (mol CO_2 /mol NH_3)	-	0.20/0.24	0.20/0.28
Net power output (MWe)	8.7	9.70	9.70
Specific reboiler duty (MJ/kg- CO_2)	N/A	6.30	4.50

Table 14: Variation of ship's speed at a capture level of 75%

Description	With capture at 85% load	With capture at 75% load
Capture level (%)	75	75
Flue gas rate (kg/s)	17.43	15.44
CO_2 content in the flue gas (kg/s)	1.35	1.3
Solvent circulation flowrate (kg/s)	140	125
Net power output (MWe)	9.7	8.7
Specific reboiler duty (MJ/kg- CO_2)	4.5	4.2

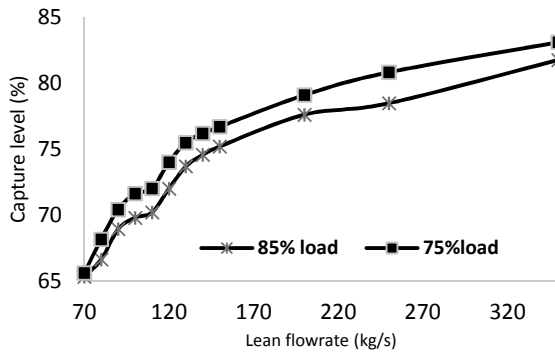


Figure 15: Effects of lean solvent flowrate on capture level

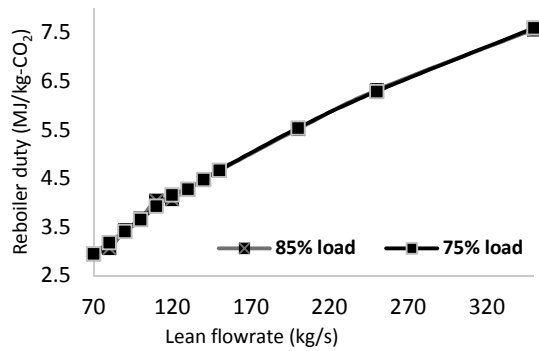


Figure 16: Effects of lean solvent flowrate on reboiler duty

3) Effect of speed change

This case simulates the effect of ship's speed change on the capture plant. Figure 15 shows the effect of the change of speed on capture level. Two engine load capacity were used at 75 and 85% to simulate speed change and to attain a high capture level, the solvent circulation flowrate was increased for each case. As the speed of the ship reduces, the quantity of the flue gas reduces effectively due to lower power requirement. In Figure 15, the lower load attained higher capture levels due to reduced flue gas flowrate at the different solvent recirculation flowrate. Also, as can be seen in Table 14, at 75% load, the amount of solvent flowrate (125 kg/s) and reboiler duty (4.2 MJ/kg-CO₂) required were lower compared to that of 85% load due to a decrease in speed and sensible heat. With 75% load, the capture level increases due to a reduced quantity of the processed flue gas compared to higher quantity at 85% load with the same solvent circulation rate. Following that, it was also observed that the required reboiler duty needed for each engine load was constant irrespective of the speed change (Figure 16), although more capture level is attained at lower speed.

6.2 Results from case studies

The total heat recovered from the ship energy system with the capture system installed was 4MW_{th} at 85% load (Figure 13), attaining a capture level of 70% with a solvent circulation flowrate of 90-100 kg/s. Flowrate beyond 100 kg/s would lead to an increase in capture rate thereby resulting in the need for additional supply of thermal energy for solvent regeneration. Utilising the waste heat thermal energy significantly reduces the thermal load required to be provided by the diesel engine. Absorption of CO₂ by NH₃ is characterised by a lower heat of reaction compared to MEA and thus requires less heat for regeneration. A CO₂ capture level of 73% with 30%wt MEA required 7.3MW_{th} [52] while 70% capture level with 4.1wt% NH₃ required approximately 4MW_{th}. This states the significance of using NH₃ and the effect on the ship's efficiency which cannot be compromised. One disadvantage of using ammonia is its volatility, but this can be avoided by using a proper abatement method [82]. Here, the NH₃ slip challenge has been reduced by the use of wash columns at the exit of both the absorber and stripper, reducing this to less than 50ppm respectively. Comparing this process to that of Luo and Wang [52], a distinct difference is seen in the type of flue gas emissions absorbed, as the latter focuses on CO₂ emissions while the former focuses on both CO₂ and SO₂ emissions. The equipment used for the CO₂ capture is the same although the SO₂ scrubbing unit and ammonium sulphite production unit are accounted for. For the re-liquefaction method when considering a CO₂ carrier, a CO₂ tank would not be necessary as re-injection into the cargo tanks could be done to limit the equipment installed on-board. Although considering a non-CO₂ carrier, a CO₂ tank would be necessary to store captured CO₂ emissions.

6.3 Analysis of storage capacity for CO₂ and ammonium sulphate

A CO₂ vessel with a capacity of 20550 m³ was considered with an ullage of 10%. The ullage is the amount of free space left intentionally in the storage tank for safety, inspection and extra capacity (Figure 17). This analysis was done in order to determine the initial liquid level of CO₂ to be filled into the storage tank when loaded at the shore. With a BOG rate of 0.2% per day (0.55 kg/s) and captured CO₂ rate of 0.74 kg/s, at a duration of 32 days, reinjection into the cargo tank will occupy 9% (5% - captured; 4% - BOG) of the space while sailing on a loaded voyage. The boil-off gas storage space would be neglected considering it originates from the tank. For a return trip (ballast voyage), assuming the capture plant is still in operation with every parameter constant, the captured CO₂ would also occupy 5% of the total cargo volume. From the above investigation, it can be concluded that when the ship is loaded on shore, the vessel should be filled with 85% of its entire volume capacity to accommodate the captured liquefied CO₂ and ullage.

The reaction of SO₂ with NH₃ leads to the formation of ammonium sulphite which can be oxidised to ammonium sulphate, a valuable product that is widely used in fertiliser production. Its global demand is on the increase and the ammonium sulphate market is expected to reach \$3.44 billion by 2022 [83]. Growing fertiliser demand on account of growing population and decreasing arable lands are key driving factors for the increase in global ammonium sulphate market. Alternatively, ammonium sulphite crystals can either be sold when the vessel get to its destination or at an intermediate stop. A safe and dry container should be used on board for storage. With the base operational parameter for capture at 85% load; the solids production rate would be 419 kg/h for an average crossing time of 32 days with the CCS system operating 60% of the time. The total mass produced is 191 tonnes. The amount accrued from the sale would be approximately \$24200 at \$127 per tonne, ignoring the costs of conversion of ammonium sulphite to sulphate, which can be readily done using the Walther process [84]. The revenues yielded from the sale can go into maintenance of the ship structure or used to build equipment needed for the Walther process conversion.

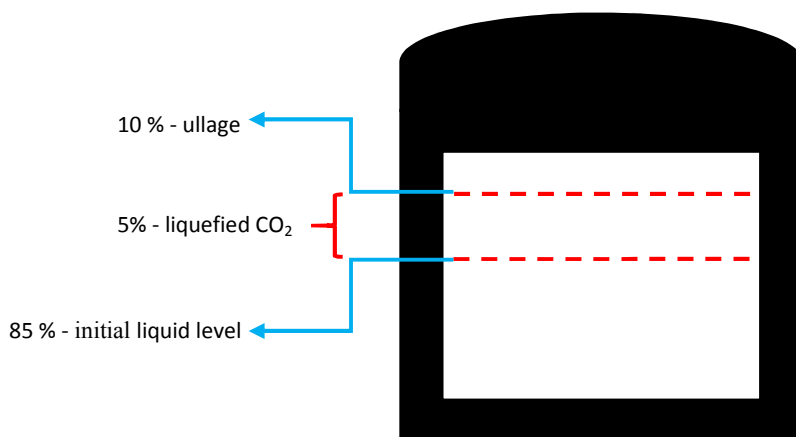


Figure 17: Cargo tank storage capacity of CO₂

7. Conclusion and future work

This study was undertaken to develop a rate-based model of an aqueous ammonia capture process integrated with a ship energy system to reduce CO₂ and SO₂ emissions simultaneously. First, the ship energy system was modelled and validated, consisting of the diesel engine and the waste heat recovery system. Secondly, a pilot-scale aqueous ammonia process was developed and validated with the Munmorah pilot data, and good agreement was seen between the pilot data and the model. It was then scaled up and modified to handle the flue gas from the ship's energy system at different operational loads. In the model, the pre-treatment column was used to reduce the sulphur

emissions before entering the absorber. Wash columns were placed at the exit of the absorber and stripper to reduce ammonia slip below 50 ppm. The ammoniated water was injected into the pre-treatment column for SO₂ removal. A capture level of 98% was obtained for SO₂.

The integrated ship model performance was analysed and three case studies were explored; one is the effect of speed change on the capture plant, another is the effect of varying the NH₃ concentration at a stable capture level and the last is the effect of changing the capture level at different speeds while sailing. It was found that the optimal point to operate the capture plant is while it is sailing, although extra power would have to be provided for electrical demand in order maintain the ship's propulsion power. The thermal energy required for solvent regeneration energy was supplied by the waste heat recovery system. The maximum heat recovered at 85% load with the CCS system in operation is 4MW_{th}, which is sufficient to capture 70% of CO₂ and 98% of SO₂. Higher capture rates would involve more power supply, thereby burning more fuel. A value-added product was generated alongside the capture process by the reaction of SO₂ and NH₃. This product could be sold once it reaches its destination.

In order to provide more information on the practicality of the integrated model, the size of each equipment should be minimised due to limited space, utility and constant movement. An economic evaluation should also be carried out to determine whether it is cheaper to install on new-built ships or as retrofits. Implementation on non-CO₂ carriers could also be considered in order to contribute to the further deployment of the application of CCS on ships.

Acknowledgement

The authors would like to acknowledge for financial support of the project from the Petroleum Technology Development Fund, Nigeria and the Engineering and Physical Sciences Research Council (EPSRC Grant No: EP/N029429/1).

References

1. IEA (2016) '20 Years of Carbon Capture and Storage - Accelerating Future Deployment', International Energy Agency, Paris, France.
2. Decarre S., Berthiaud J., Butin N., Guillaume-Combecave JL. 'CO₂ maritime transportation'. International Journal of Greenhouse Gas Control; 2010; 4(5): 857–864.
3. Yoo, B. Y., Lee, S. G., Rhee, K. P., Na, H. S. and Park, J. M. (2011) 'New CCS system integration with CO₂ carrier and liquefaction process', Energy Procedia, 4, 2308–2314.
4. Aspelund A., Mølnvik MJ., De Koeijer G. 'Ship Transport of CO₂- Technical Solutions and Analysis of Costs, Energy Utilization, Exergy Efficiency and CO₂ Emissions'. Chemical Engineering Research and Design. 2006; 84(9): 847–855
5. Neele, F., Haugen, H. A. and Skagestad, R. (2014) 'Ship transport of CO₂ - Breaking the CO₂-EOR deadlock', Energy Procedia, 63, 2638–2644
6. Vermeulen, T. N. (2011) 'Knowledge sharing report – CO₂ Liquid Logistics Shipping Concept (LLSC): Overall Supply Chain Optimization', Global CCS Institute, Anthony Veder, Vopak
7. Omata A. and Hattori K (2011) 'Final report: Preliminary feasibility study on CO₂ carrier for ship-based CCS', Chiyoda Corporation, Global CCS Institute.
8. Roussanaly, S., Jakobsen, J. P., Hognes, E. H. and Brunsvold, A. L. (2013) 'Benchmarking of CO₂ transport technologies: Part I—Onshore pipeline and shipping between two onshore areas', International Journal of Greenhouse Gas Control. 584–594.
9. Elementenergy. 'Shipping CO₂ – UK Cost Estimation Study'. Element energy, United Kingdom
10. Veronika E., Ivar S.A I., Berntsen T., Collins WJ., Corbett JJ., Oyvind E., et al. 'Transport impacts on atmosphere and climate: Shipping'. Atmospheric Environment; 2010; 44(37): 4735–4771.
11. WHO. 'Burden of disease from the joint effects of Household and Ambient Air Pollution for 2012'. World Health Organisation; 2014
12. IMO 'Greenhouse Gas Emissions'. International Maritime Organisation. 2018. Available at: <http://www.imo.org/en/OurWork/Environment/PollutionPrevention/AirPollution/Pages/GHG-Emissions.aspx> (Accessed: 16 June 2018)

13. IEA. 'Energy Technology Perspectives 2012 - Pathways to Clean Energy System'. International Energy Agency. France; 2012
14. Andersson K., Brynolf S., Lindgren JF., Wilewska-Bien M. 'Shipping and the Environment: Improving Environmental Performance in Marine Transportation'. 2016. Gothenburg, Sweden: Springer pp 190-191
15. IMO. 'Sulphur oxides (SOx) and Particulate Matter (PM) – Regulation 14'. International Maritime Organisation. 2018. Available at: [http://www.imo.org/en/OurWork/Environment/PollutionPrevention/AirPollution/Pages/Sulphur-oxides-\(SOx\)---Regulation-14.aspx](http://www.imo.org/en/OurWork/Environment/PollutionPrevention/AirPollution/Pages/Sulphur-oxides-(SOx)---Regulation-14.aspx) (Accessed: 16 June 2018)
16. Bouman EA., Lindstad E., Rialland AI., Strømman AH. 'State-of-the-art technologies, measures, and potential for reducing GHG emissions from shipping – A review'. Transportation Research Part D: Transport and Environment. 2017; 52: 408–421.
17. Corbett, J. J. (2003) 'Updated emissions from ocean shipping', Journal of Geophysical Research, 108(D20), 4650.
18. Smith, T. W. P., Jalkanen, J. P., Anderson, B. A., Corbett, J. J., Faber, J., Hanayama, S., O'Keeffe, E., Parker, S., Johansson, L., Aldous, L., Raucchi, C., Traut, M., Ettinger, S., Nelissen, D., Lee, D. S., Ng, S., Agrawal, A., Winebrake, J., J.Hoen, M., Chesworth, and Pandey, A. 'Third IMO GHG Study' 2014. International Maritime Organisation
19. DNV GL. 'Assessment of Selected Alternative Fuels and Technologies' DNV.GL-Maritime. 2018.
20. Gerd W. 'Alternative fuels in shipping' (Video webinar). DNV.GL-Maritime; 2018. Available at <https://www.dnvgl.com/maritime/webinars-and-videos/on-demand-webinars/alternative-fuels-in-shipping.html>
21. Songolzadeh M., Soleimani M., Takht Ravanchi M., Songolzadeh R. 'Carbon dioxide separation from flue gases: A technological review emphasizing reduction in greenhouse gas emissions'. The Scientific World Journal. 2014.
22. Puxty G., Wei SCC., Feron P., Meuleman E., Beyad Y., Burns R., et al. 'A novel process concept for the capture of CO₂ and SO₂ using a single solvent and column'. Energy Procedia; 2014; 63: 703–714.
23. Asif M., Kim W-S. 'Modelling and simulation of the combined removal of SO₂ and CO₂ by aqueous ammonia'. Greenhouse Gases: Science and Technology. August 2014; 4(4): 509–527.
24. Yu H., Li L., Maeder M., Li K., Tade M. 'Development of an Aqueous Ammonia Based PCC Technology for Australian Conditions Process modelling of combined SO₂ and CO₂ capture using aqueous ammonia'. 2015. CSIRO Energy Technology, Australia.
25. James TY., Henry WP. US007255842B1: 'Multi-component removal in flue gas by aqua ammonia'. United State; 2007.
26. Eli G. US 2008/0072762 A1: 'Ultra cleaning of combustion gas including the removal of CO₂'. United States; 2008.
27. Resnik KP., Yeh JT., Pennline HW. 'Aqua ammonia process for simultaneous removal of CO₂, SO₂ and NO_x'. International Journal of Environmental Technology and Management. 2004; 4(1–2): 89–104.
28. Zhang M., Guo Y. 'Process simulations of NH₃ abatement system for large-scale CO₂ capture using aqueous ammonia solution'. International Journal of Greenhouse Gas Control; 2013; 18: 114–127.
29. Puxty G., Rowland R., Attalla M. 'Comparison of the rate of CO₂ absorption into aqueous ammonia and monoethanolamine'. Chemical Engineering Science. 2010. pp. 915–922.
30. Dong R., Lu H., Yu Y., Zhang Z. 'A feasible process for simultaneous removal of CO₂, SO₂ and NO_x in the cement industry by NH₃ scrubbing'. Applied Energy; 2012; 97: 185–191.
31. A.van de Runstraat., M.R. Abu-Zahra., P.H.M. Feron. 'CO₂ removal by aqueous ammonia scrubbing'. TNO Science and Industry The Netherlands; 2007
32. Ciferno JP., DiPietro P., Tarka T. 'An economic scoping study for CO₂ capture using aqueous ammonia'. Final Report, National Energy Technology Laboratory, US Department of Energy, Pittsburgh, PA. 2005.
33. Lombardo G., Agarwal R., Askander J. 'Chilled Ammonia Process at Technology Center Mongstad – First Results'. Energy Procedia; 2014; 51: 31–39.
34. Darde V., Thomsen K., van Well WJM., Stenby EH. 'Chilled ammonia process for CO₂ capture'. Energy Procedia; 2009; 1(1): 1035–1042.
35. McLarnon CR., Duncan JL. 'Testing of Ammonia Based CO₂ Capture with Multi-Pollutant Control

Technology'. *Energy Procedia*. Elsevier; 2009; 1(1): 1027–1034.

36. Yu H., Qi G., Wang S., Morgan S., Allport A., Cottrell A., et al. 'Results from trialling aqueous ammonia-based post-combustion capture in a pilot plant at Munmorah Power Station: Gas purity and solid precipitation in the stripper'. *International Journal of Greenhouse Gas Control*; 2012; 10: 15–25.
37. Yu H., Morgan S., Allport A., Cottrell A., Do T., McGregor J., et al. 'Results from trialling aqueous NH₃ based post-combustion capture in a pilot plant at Munmorah power station': Absorption. *Chemical Engineering Research and Design*. Institution of Chemical Engineers; 2011; 89(8): 1204–1215.
38. Li K., Yu H., Qi G., Feron P., Tade M., Yu J., et al. 'Rate-based modelling of combined SO₂ removal and NH₃ recycling integrated with an aqueous NH₃-based CO₂ capture process'. *Applied Energy*. 2015; 148: 66–77.
39. Li X., Hagaman E., Tsouris C., Lee JW. 'Removal of carbon dioxide from flue gas by ammonia carbonation in the gas phase'. *Energy and Fuels*. 2003; 17(1): 69–74.
40. Niu Z., Guo Y., Zeng Q., Lin W. 'Experimental studies and rate-based process simulations of CO₂ absorption with aqueous ammonia solutions'. *Industrial and Engineering Chemistry Research*. 2012; 51(14): 5309–5319.
41. Hanak DP., Biliyok C., Manovic V. 'Rate-based model development, validation and analysis of chilled ammonia process as an alternative CO₂ capture technology for coal-fired power plants'. *International Journal of Greenhouse Gas Control*; 2015; 34: 52–62.
42. Han C. 'Strategies to Reduce Air Pollution in Shipping Industry'. *The Asian Journal of Shipping and Logistics*. 2010; 26(1): 7–29.
43. Bergqvist R., Turesson M., Weddmark A. 'Sulphur emission control areas and transport strategies - the case of Sweden and the forest industry'. *European Transport Research Review*. 2015; 7(2).
44. Lloyd's Register. 'Understanding exhaust gas treatment systems. Guidance for ship owners and operators'. 2012. Lloyd's Register Engineering Services, United Kingdom, London.
45. Boer E Den. 'Scrubbers – An economic and ecological assessment'. 2015. CE Delft, Delft.
46. Kjølholt J., Aakre S., Jürgensen C., Lauridsen J. 'Assessment of possible impacts of scrubber water discharges on the marine environment'. 2012. Danish Ministry of the Environment, Environmental Protection Agency
47. Thomson H., Corbett JJ., Winebrake JJ. 'Natural gas as a marine fuel'. *Energy Policy*; 2015; 87: 153–167.
48. Eide MS., Longva T., Hoffmann P., Endresen O., Dalsoren SB. 'Future cost scenarios for reduction of ship CO₂ emissions'. *Maritime Policy & Management*. 2011; 38(1): 11–37.
49. J.J Sweeney. 'A comprehensive programme for shipboard energy conservation in shipboard energy conservation'. Society of Naval Architects and Marine Engineers. 1980
50. DNV and PSE. 'News - Press releases - DNV-PSE CCS Report'. 2013. Available at <https://www.psenderprise.com/news/news-press-releases-dnv-pse-ccs-report> (Accessed: 16 September 2018). Delft University of Technology.
51. Zhou P., Wang H. 'Carbon capture and storage - Solidification and storage of carbon dioxide captured on ships'. *Ocean Engineering*; 2014; 91: 172–180.
52. Luo X., Wang M. 'Study of solvent-based carbon capture for cargo ships through process modelling and simulation'. *Applied Energy*; 2017; 195: 402–413.
53. Van den Akker J. 'Carbon Capture Onboard LNG Fueled Vessels - A feasibility study'. Master of Science in marine technology; Delft University of Technology; 2017.
54. Hasan MMF., Zheng AM., Karimi IA. 'Minimizing boil-off losses in liquefied natural gas transportation'. *Industrial and Engineering Chemistry Research*. 2009; 48(21): 9571–9580.
55. Gerdsmeyer K-D., Isalski W. 'On-board reliquefaction for LNG ships'. Tractebel Gas Engineering, Gastech Gastech 2005.
56. Jeon SH., Choi YU., Kim MS. 'Review on Boil-Off Gas (BOG) Re-Liquefaction System of Liquefied CO₂ Transport Ship for Carbon Capture and Sequestration (CCS)'. *International Journal of Air-Conditioning and Refrigeration*. 2016; 24(3): 1–10.
57. Aspelund, A. and Jordal, K. (2007) 'Gas conditioning-The interface between CO₂ capture and transport', *International Journal of Greenhouse Gas Control*, 1(3), 343–354.
58. Jeon SH., Kim MS. 'Compressor selection methods for multi-stage re-liquefaction system of liquefied CO₂

- transport ship for CCS'. *Applied Thermal Engineering*; 2015; 82: 360–367.
59. Lee Y., Baek KH., Lee S., Cha K., Han C. 'Design of boil-off CO₂ re-liquefaction processes for a large-scale liquid CO₂ transport ship'. *International Journal of Greenhouse Gas Control*; 2017; 67: 93–102.
 60. Barrio M., Aspelund A., Weydahl T., Sandvik TE., Wongraven LR., Krogstad H., et al. 'Ship-based transport of CO₂'. *Greenhouse Gas Control Technologies*. 2005. pp. 1655–1660.
 61. Wartsila. 'Wärtsilä 46F Product Guide'. 2017. Wartsila Engines
 62. Navigator Aries. 'Pocket Plan 20,550CBM LPG Carrier'. 2018. Available at <https://www.navigatorgas.com/>
 63. Abdul Jameel AG., Elbaz AM., Emwas A-H., Roberts WL., Sarathy SM. 'Calculation of Average Molecular Parameters, Functional Groups, and a Surrogate Molecule for Heavy Fuel Oils Using 1H and 13C Nuclear Magnetic Resonance Spectroscopy'. *Energy & Fuels*. 2016; 30(5): 3894–3905.
 64. MAN Diesel & Turbo. 'Thermo Efficiency System (TES) - for Reduction of Consumption and CO₂ Emission' 2014
 65. Singh DV., Pedersen E. 'A review of waste heat recovery technologies for maritime applications'. *Energy Conversion and Management*; 2016; 111(2016): 315–328.
 66. Ports.com. 'Port of Ardalstangen, Norway to Mawei Port, China - Sea route & distance - ports.com'. 2018. Available at: <http://ports.com/sea-route/>
 67. Gassnova. 'Feasibility study for full-scale CCS in Norway'. Gassnova. Ministry of Petroleum and Energy. Norway; 2016. Available at: DOI:10.1007/s00253-011-3828-8
 68. Wigforss J. 'Benchmarks and measures for better fuel efficiency'. Chalmers University of Technology, Sweden; 2012.
 69. Zhang M., Guo Y. 'Process simulations of large-scale CO₂ capture in coal-fired power plants using aqueous ammonia solution'. *International Journal of Greenhouse Gas Control*; 2013; 16: 61–71.
 70. Bravo J., Rocha J., Fair J. 'Mass transfer in gauze packings'. *Hydrocarb Process*. 1985; 64: 91–95.
 71. Chilton TH., Colburn AP. 'Mass Transfer (Absorption) Coefficients: Prediction from Data on Heat Transfer and Fluid Friction' *Industrial and Engineering Chemistry*. 1934; 26(11): 1183–1187.
 72. Aspen Tech. 'Rate-based model of the CO₂ capture process by NH₃ using Aspen Plus'. Burlington, MA USA; 2010
 73. Ermatchkov V., Kamps ÁPS., Maurer G. 'The chemical reaction equilibrium constant and standard molar enthalpy change for the reaction {2HSO₃(aq) ⇌ S₂O₂⁻⁵(aq) + H₂O(1)}: A spectroscopic and calorimetric investigation'. *Journal of Chemical Thermodynamics*. 2005; 37(2): 187–199.
 74. Pinsent BRW., Roughton FJW., Pearson L. 'The kinetics of combination of carbondioxide with hydroxide ions'. 1956; 52: 1512–1520.
 75. Pinsent BRW., Pearson L., Roughton FJW. 'The kinetics of combination of carbon dioxide with ammonia'. *Transactions of the Faraday Society*. 1956; 52: 1594–1598.
 76. Jilvero H., Normann F., Andersson K., Johnsson F. 'The rate of CO₂ absorption in ammonia-implications on absorber design'. *Industrial and Engineering Chemistry Research*. 2014. pp. 6750–6758.
 77. Kister H. 'Distillation Design'. United States of America McGraw-Hill; 1992. Pp 722
 78. Johann G S., James R F. 'Distillation Principles and Practices'. New York: Wiley VCH
 79. Sinnott RK. 'Chemical Engineering Design. Coulson and Richardson's Chemical Engineering Volume 6'. Fourth edition, Elsevier, 2005; pp 587-624
 80. Yoo B. 'The development and comparison of CO₂ BOG re-liquefaction processes for LNG fueled CO₂ carriers'. *Energy*. 2017; 127: 186–197.
 81. Zhang M., Guo Y. 'Rate based modeling of absorption and regeneration for CO₂ capture by aqueous ammonia solution'. *Applied Energy*; 2013; 111(2013): 142–152.
 82. Niu Z., Guo Y., Zeng Q., Lin W. 'A novel process for capturing carbon dioxide using aqueous ammonia. *Fuel Processing Technology*'; 2013; 108: 154–162.
 83. Grand View Research. 'Ammonium Sulfate Market Size, Research | Industry Report, 2012-2022'. 2016. Available at: <https://www.grandviewresearch.com/industry-analysis/ammonium-sulfate-market> (Accessed: 1 October 2018)
 84. Schulte W. Walther Process. Sulphur Dioxide and Nitrogen Oxides in Industrial Waste Gases: Emission,

Legislation and Abatement. eds. Springer, Dordrecht; 1991. pp. 167–181.

CO₂/SO₂ emission reduction in CO₂ shipping infrastructure

Awoyomi, Adeola

2019-06-04

Attribution-NonCommercial-NoDerivatives 4.0 International

Awoyomi A, Patchigolla K, Anthony EJ. (2019) CO₂/SO₂ emission reduction in CO₂ shipping infrastructure. International Journal of Greenhouse Gas Control, Volume 88, September 2019, pp. 57-70

<https://doi.org/10.1016/j.ijggc.2019.05.011>

Downloaded from CERES Research Repository, Cranfield University